

# *Ab initio* investigation of the exchange interactions in $\text{Bi}_2\text{Fe}_4\text{O}_9$ : The Cairo pentagonal lattice compound

Z.V. Pchelkina<sup>1,2,\*</sup> and S.V. Streltsov<sup>1,2,†</sup>

<sup>1</sup>*Institute of Metal Physics, S.Kovalevskoy St. 18, 620990 Ekaterinburg, Russia*

<sup>2</sup>*Ural Federal University, Mira St. 19, 620002 Ekaterinburg, Russia*

(Dated: September 13, 2018)

We present the *ab initio* calculation of the electronic structure and magnetic properties of  $\text{Bi}_2\text{Fe}_4\text{O}_9$ . This compound crystallizes in the orthorhombic crystal structure with the  $\text{Fe}^{3+}$  ions forming the Cairo pentagonal lattice implying strong geometric frustration. The neutron diffraction measurements reveal nearly orthogonal magnetic configuration, which at first sight is rather unexpected since it does not minimize the total energy of the pair of magnetic ions coupled by the Heisenberg exchange interaction. Here we calculate the electronic structure and exchange integrals of  $\text{Bi}_2\text{Fe}_4\text{O}_9$  within the LSDA+U method. We obtain three different in-plane ( $J_3=36$  K,  $J_4=73$  K,  $J_5=23$  K) and two interplane ( $J_1=10$  K,  $J_2=12$  K) exchange parameters. The derived set of exchange integrals shows that the realistic description of  $\text{Bi}_2\text{Fe}_4\text{O}_9$  needs a more complicated model than the ideal Cairo pentagonal lattice with only two exchange parameters in the plane. However, if one takes into account only two largest exchange integrals, then according to the ratio  $x \equiv J_3/J_4=0.49 < \sqrt{2}$  (a critical parameter for the ideal Cairo pentagonal lattice, see. Ref. 1) the ground state should be the orthogonal magnetic configuration in agreement with experiment. The microscopic origin of different exchange interactions is also discussed.

PACS numbers: 75.25.-j, 71.20.-b, 75.30.Et

## I. INTRODUCTION

Until D. Shechtman discover quasicrystals (the Nobel Prize in Chemistry in 2011) it was thought that it is impossible to pack atoms into a regular lattice and obey a pentagonal symmetry. [2] This type of the symmetry is not rare in the nature. It can be found in wildflowers and many sea dwellers as well as in scale of a fir cone and a pineapple. The only known naturally occurring quasicrystal phase is the icosahedrite ( $\text{Al}_{63}\text{Cu}_{24}\text{Fe}_{13}$ ) found in the Koryak Mountains in Russia. The quasicrystals reveal a new class of the organization of the matter with regular but non-periodic lattice. Such patterns have been known in the mathematics since antiquity, and medieval Islamic artists made decorative, non-repeating tessellation (the Cairo pentagonal mosaic).

Such an exotic and rare structure is the subject of a keen interest from both experimental and theoretical point of view. As the number of bonds per elemental “brick” in the pentagonal lattice is odd the nearest neighbor antiferromagnetic (AFM) interactions would lead to the geometrical frustration. At present the most studied 2D magnetic frustrated lattice is the triangular one consisting of regular polygons with equal nearest neighbor exchange interactions. Contrary to the triangles it is impossible to fill the plane with regular pentagons, the “bricks” of another shape are needed like in the Penrose lattice. Such a tessellation however, can be constructed using non-regular pentagons as in the case of the Cairo

pentagonal lattice.

The comprehensive analytical and numerical investigation of the antiferromagnetic Heisenberg model on the Cairo pentagonal lattice have been recently presented. [1] A simple pentagonal lattice studied in Ref. 1 consists of two inequivalent sites with three and four nearest neighbors (see Fig. 2 and Fig. 1 in Ref. 1). It has two types of the nonequivalent bonds, which connect threefold sites with each other ( $J_{33}$  exchange constant) and threefold sites with fourfold ones ( $J_{43}$  exchange path). Such a Cairo pentagonal lattice has a square Bravais lattice and the unit cell containing four fourfold- and two threefold-coordinated sites. The phase diagram of the AFM Heisenberg model was obtained as a function of the ratio  $x \equiv J_{43}/J_{33}$  and spin  $S$ . In the classical limit (large  $S$ ) three magnetic phases have been found: 1) the phase, where the spins on the neighboring sites are orthogonal to each other ( $x < \sqrt{2}$ ), 2) a collinear 1/3-ferrimagnetic phase ( $x > 2$ ) and 3) an intermediate mixed phase ( $\sqrt{2} < x < 2$ ) which is a combination of 1) and 2).[1]

At present there are known only two complex iron oxides which represent the physical realization of magnetic Cairo pentagonal lattice, namely  $\text{Bi}_2\text{Fe}_4\text{O}_6$  [1] and  $\text{Bi}_4\text{Fe}_5\text{O}_{13}\text{F}$ . [3]  $\text{Bi}_2\text{Fe}_4\text{O}_6$  can be obtained as a by-product in the synthesis of the multiferroic  $\text{BiFeO}_3$  and seems to reveal multiferroic properties by itself. [4] It is also regarded as a perspective material for the semiconductor gas sensors. [5]

$\text{Bi}_2\text{Fe}_4\text{O}_6$  crystallizes in a complex orthorhombic structure [6, 7] with the space group  $Pbam$  (No. 55). It has two formula units in the unit cell and two nonequivalent iron atoms  $\text{Fe}_t$  and  $\text{Fe}_o$  occupying the tetrahedral and octahedral positions, correspondingly (see Fig. 1). The

---

\*Electronic address: pzv@ifmlrs.uran.ru

†Electronic address: streltsov.s@gmail.com

edge-sharing  $\text{Fe}_o\text{O}_6$  octahedra form chains along the  $c$  direction and these chains are bind by the corner-sharing  $\text{Fe}_t\text{O}_4$  tetrahedra and Bi atoms.  $\text{Fe}_t$  occupies aforementioned threefold-coordinated sites, while  $\text{Fe}_o$  - fourfold.

The magnetic measurements on the single crystals were performed in Ref. 7. At high temperature a Curie-Weiss fitting of the magnetic susceptibility gives the paramagnetic temperature  $\theta_p \approx -1670$  K and the effective magnetic moment  $\mu_{eff} = 6.3(3)\mu_B$  per iron atom in agreement with value  $5.9\mu_B$  corresponding to  $S=5/2$  of the  $\text{Fe}^{3+}$  ions. The long range magnetic order with  $T_N=238$  K sets in at much lower temperature indicating the presence of magnetic frustrations in the systems. In the unusual nearly orthogonal magnetic structure at low temperatures the moments on all the iron atoms lying in the  $(a,b)$  plane. The  $\text{Fe}_o$  spins form four orthogonal sublattices while the  $\text{Fe}_t$  spins align antiferromagnetically with each other (see Fig. 2).

In contrast to the perfect Cairo lattice model stud-

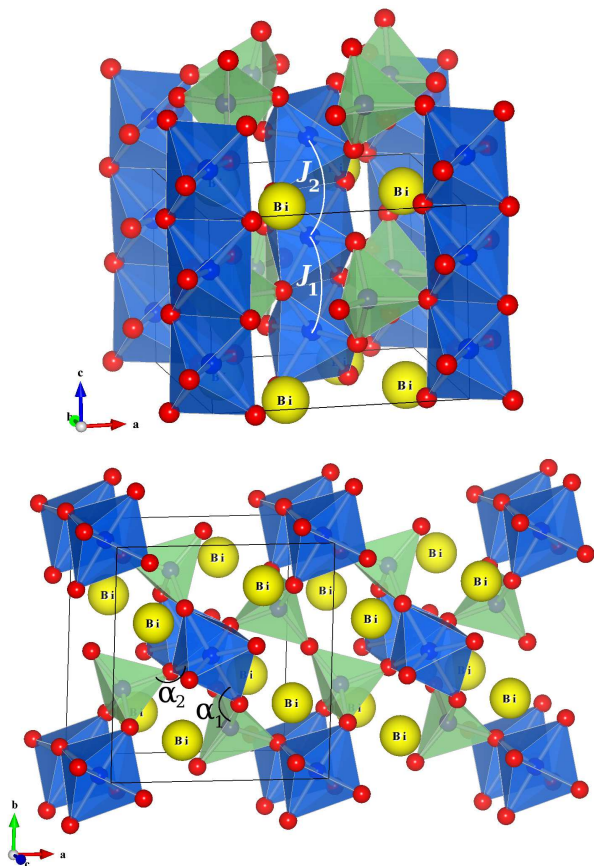


FIG. 1: (color online). The crystal structure of  $\text{Bi}_2\text{Fe}_4\text{O}_9$  along the  $c$  axis (upper panel) and in the  $ab$  plane (lower panel). There are two types of the Fe ions:  $\text{Fe}_o$  is placed in the oxygen octahedra (blue), while  $\text{Fe}_t$  is in the ligand tetrahedra (green). O and Bi are shown as red and yellow balls respectively.  $J_1$  and  $J_2$  are the interplane exchange interactions. We use VESTA software [8] for visualization.

ied in Ref. 1 the real orthorhombic crystal structure of  $\text{Bi}_2\text{Fe}_4\text{O}_9$  has few distinct features. Namely, each pentagonal unit cell contains seven sites because there are two  $\text{Fe}_o$  ions in the center of the unit cell (Fig. 1) with different coordinate along the  $c$  axis, while the ideal structure has only one. Hence, for the realistic treatment of the magnetic interactions one needs to calculate at least five different exchange constants, which can hardly be done reliably by fitting the model solutions of the Heisenberg Hamiltonian to the magnetic susceptibility or other experimental observables. Such a fitting allows however to estimate the ratio between some of the exchange integrals. [7]

In this paper we present the *ab initio* calculation of the exchange constants in  $\text{Bi}_2\text{Fe}_4\text{O}_9$ , compare the result obtained with available theoretical and experimental data, show that this system cannot be considered as a realization of the perfect Cairo pentagonal lattice, and discuss the microscopic mechanisms, which define the strength of different magnetic interactions.

## II. CALCULATION DETAILS

We used the linearized muffin-tin orbitals method (LMTO) [9] with the von Barth-Hedin version of the exchange correlation potential [10] to calculate the electronic and magnetic properties of  $\text{Bi}_2\text{Fe}_4\text{O}_9$ . In order to take into account strong electronic correlations on the Fe sites the LSDA+U approximation was applied [11] with the on-site Coulomb repulsion parameter  $U=4.5$  eV and the intra-atomic Hund's rule exchange  $J_H=1$  eV. [12, 13]

The Liechtenstein's exchange interaction parameter (LEIP) calculation procedure [14] was used to find the inter-site exchange constants for the Heisenberg model written as

$$H = \sum_{ij} J_{ij} \vec{S}_i \vec{S}_j, \quad (1)$$

where each site in the summation is counted twice. According to this method, exchange constants  $J$  can be calculated as the second derivative of the total energy variation at small spin rotation. This allows to (1) calculate all  $J$  in one magnetic configuration and (2) check whether a given spin structure corresponds to the ground state or spins on some of the sites must be reversed. The later is seen from the sign of  $J$ , calculated in the LEIP method: if  $J$  is negative (i.e. the second derivative of the total energy is negative) then the total energy has a minimum for a given magnetic order, but if  $J$  is positive then one should recalculate the exchange constant for a given bond in another spin structure, since the curvature of the total energy surface and hence the value of  $J$  in general can be different for minima and maxima.

For the calculation of the exchange constants between the tetrahedral and octahedral Fe ( $J_3$  and  $J_5$  in Fig. 2) we used the magnetic configuration, where the spins on these bonds are antiferromagnetically coupled, but then

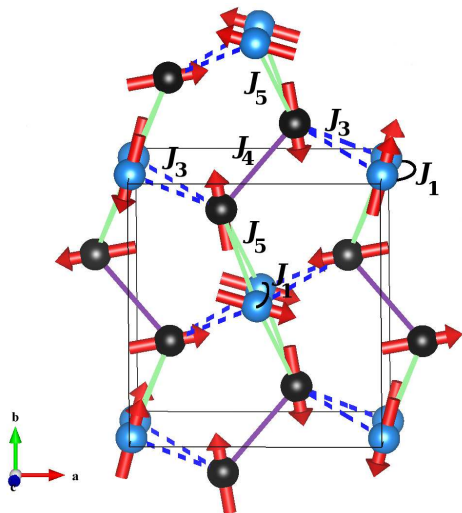


FIG. 2: (color online). The pentagonal magnetic lattice of  $\text{Bi}_2\text{Fe}_4\text{O}_9$  ( $ab$  projection) together with exchange interactions notations. The spins on each site are the same ( $S=5/2$ ), but the sites have different surrounding: the octahedral  $\text{Fe}_o$  ions are shown in blue, the tetrahedral  $\text{Fe}_t$  ions - in black. The bonds between tetrahedral  $\text{Fe}_t$  are violet ( $J_4$ ), while between octahedral  $\text{Fe}_o$  and tetrahedral  $\text{Fe}_t$  are green ( $J_5$ ) and blue ( $J_3$ , dotted line). The spin orientation represents the experimentally detected magnetic structure from Ref. [7]. In the case of ideal Cairo pentagonal lattice  $\text{Fe}_t$  ions correspond to the threefold-coordinated sites, while  $\text{Fe}_o$  correspond to the fourfold-coordinated sites. Hence, in the notation of Ref. 1:  $J_4 \rightarrow J_{33}$  and  $J_3 = J_5 \rightarrow J_{43}$ .

the pairs of two tetrahedral  $\text{Fe}_t$  ( $J_4$ ) turn out to be ferromagnetically ordered. The calculation using the LEIP method shows that the signs for  $J_3$  and  $J_5$  are correct (negative) for this order, but the direction of one of the spins forming  $J_4$  path must be reversed. By checking few other magnetic configurations where spins on the  $\text{Fe}_t$ - $\text{Fe}_t$  bond were antiferromagnetically ordered we found that in this case the LEIP method gives negative  $J_4$  and its value is the same in these calculations. The same procedure was repeated for the interplane exchange coupling  $J_1$  and  $J_2$ . Since the signs provided by the LEIP procedure does not correspond to the usual conventions, in the following the positive (negative) exchange constants will mean antiferromagnetic (ferromagnetic)  $J$  according to the Heisenberg model presented in Eq. (1).

The crystal structure was taken from Ref. 6 and is shown in Fig. 1. The mesh of 144  $\mathbf{k}$ -points was used in the course of the self consistency.

### III. RESULTS

The total and partial density of states (DOS) obtained in the LSDA+U calculation for the magnetic configuration, where all pairs of  $\text{Fe}_t$ - $\text{Fe}_o$  are antiferromagnetically ordered are presented in Fig. 3. The DOS obtained for

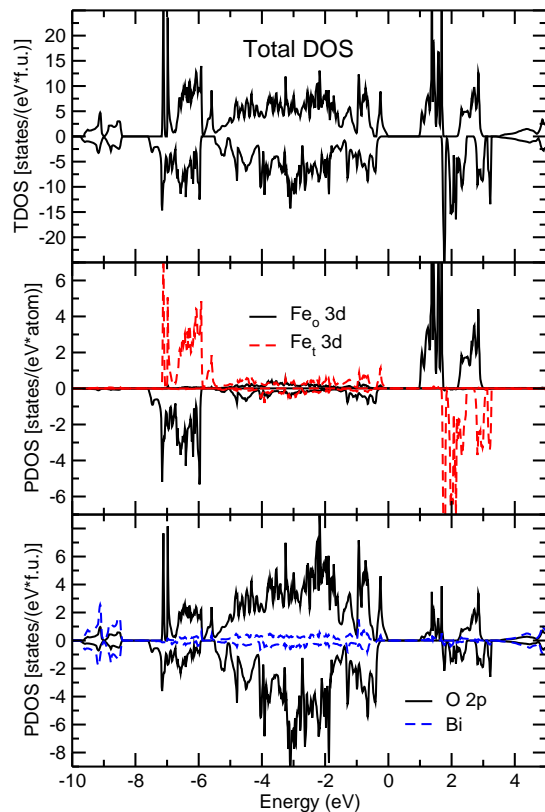


FIG. 3: (color online). The total and partial density of states plot obtained in the LSDA+U calculation for the magnetic configuration, where all  $\text{Fe}_t$  and  $\text{Fe}_o$  are antiferromagnetically ordered. The positive (negative) values correspond to the spin up (down). The Fermi energy is in zero.

other magnetic structures is quite similar. The top of the valence band is mostly defined by the O 2p states, while the bottom of the conduction band is formed by the Fe 3d (spin minority) states. So that  $\text{Bi}_2\text{Fe}_4\text{O}_9$  must be classified as a charge transfer insulator. [15] The band gap varies from 0.97 eV to 1.28 eV depending on the magnetic configuration under consideration. The values of the spin moments are slightly reduced from  $5 \mu_B$  expected for the  $\text{Fe}^{3+}$  ions with  $S = 5/2$  due to the hybridization effects and equal 3.9-4.0  $\mu_B$ .

There are three different types of the exchange coupling in the  $ab$  plane according to our calculations (see Fig. 2). The largest is  $J_4 = 73$  K for the pair of the tetrahedral  $\text{Fe}_t$ . There are also two  $J_5 = 23$  K and two  $J_3 = 36$  K both between the octahedral and tetrahedral Fe ions. The main mechanism for all of them is the superexchange via oxygen ion shared by two  $\text{FeO}_{6(4)}$  polyhedra. The values of these three exchange constants are different because of the quite different geometry of

the Fe-O-Fe bonds and the ligand polyhedra surrounding each Fe ion.

The exchange constant between two tetrahedral  $\text{Fe}_t$  ions is the largest, because of the strong  $t_{2g}/t_{2g}$  exchange coupling. The  $t_{2g}$  orbitals are directed as much as possible to the oxygens in the tetrahedral case and three  $t_{2g}$  orbitals on each  $\text{Fe}_t$  site take part in a strong superexchange with the  $2p$  orbitals of a common O, via the  $180^\circ$  Fe-O-Fe bond. The direct calculation shows that  $J_4^{t_{2g}/t_{2g}} = 50$  K, whereas  $J_4^{t_{2g}/e_g} = 16$  K and  $J_4^{e_g/e_g} = 7$  K.

If the coordinate system is chosen in a way shown in Fig. 4, it's convenient to work not with the conventional  $p_x$ ,  $p_y$ , and  $p_z$  orbitals, but with  $p_\sigma = (p_x + p_y + p_z)/\sqrt{3}$ ,  $p_1 = (p_x - p_y)/\sqrt{2}$ , and  $p_2 = (p_x + p_y - 2p_z)/\sqrt{6}$ . Then the largest  $p-d$  hopping in the tetrahedra will be between  $p_\sigma$  and any of the  $t_{2g}$  orbitals (different  $p-t_{2g}$  hopping matrix elements in the case of a regular tetrahedron are calculated in Tab. I with the use of the Slater-Koster parametrization [16]). Hence the largest contribution to the total exchange interaction between two tetrahedral  $\text{Fe}_t$  will be the superexchange via the  $p_\sigma$  orbital:

$$J_{tt}^{t_{2g}/p_\sigma/t_{2g}} \sim 9 \frac{(t_{p_\sigma t_{2g}}^{tet})^2 (t_{p_\sigma t_{2g}}^{tet})^2}{U \Delta_{CT}^2}, \quad (2)$$

where  $\Delta_{CT}$  is the charge transfer energy (energy of the excitation from the O  $2p$  orbitals to the  $3d$  shell of a transition metal ion, in our case,  $\text{Fe}^{3+}(d^5)\text{O}^{2-}(2p^6) \rightarrow \text{Fe}^{2+}(d^6)\text{O}^-(2p^5)$ ), [15] and  $t_{p_\sigma t_{2g}}^{tet}$  is the hopping matrix element between  $p_\sigma$  and one of the  $t_{2g}$  orbitals in the  $\text{FeO}_4$  tetrahedron. Factor 9 comes from the number of the different  $t_{2g}$  orbitals on each site. In the case of the  $t_{2g}/e_g$  exchange interaction this prefactor will be smaller, so are the hoppings integrals (there will be mostly  $t_{pd\pi}$  hoppings, which are approximately two times smaller than  $t_{pd\sigma}$  [17]).

It is interesting that Eq. (2) can be rewritten in a more useful form if one will use a basis of the trigonal-like [18] orbitals also for the  $3d$  states, i.e.  $a_{1g} = (d_{xy} + d_{yz} + d_{zx})/\sqrt{3}$ ,  $t_1 = (d_{yz} - d_{zx})/\sqrt{2}$ , and  $t_2 = (d_{yz} + d_{zx} - 2d_{xy})/\sqrt{6}$ . Then all  $t_{pd}$  hopping parameters will be zero except  $t_{p_\sigma a_{1g}} = t_{pd\sigma}$ ,  $t_{p_1 t_1} = t_{p_2 t_2} = -t_{pd\pi}/\sqrt{3}$  and there will be only two contributions to the exchange between the  $t_{2g}$  orbitals coming from the  $a_{1g}$  orbitals:

$$J_{tt}^{a_{1g}/p_\sigma/a_{1g}} \sim \frac{(t_{pd\sigma}^{tet})^4}{U \Delta_{CT}^2}, \quad (3)$$

and from the  $t_1$  and  $t_2$  orbitals

$$J_{tt}^{t_1/p_\sigma/t_1} \sim \frac{2(t_{pd\pi}^{tet})^4}{9U \Delta_{CT}^2}. \quad (4)$$

Using the estimation of the interatomic matrix elements [17] it's easy to find that the ratio

$$\frac{J_{tt}^{a_{1g}/p_\sigma/a_{1g}}}{J_{tt}^{t_1/p_\sigma/t_2}} \sim 100, \quad (5)$$

TABLE I: The values of the  $p-d$  hopping matrix elements ( $t_{pd}$ ) between the  $d$  and  $p$  orbitals ( $p_\sigma = (p_x + p_y + p_z)/\sqrt{3}$ ,  $p_1 = (p_x - p_y)/\sqrt{2}$ , and  $p_2 = (p_x + p_y - 2p_z)/\sqrt{6}$ ) in the case of the regular  $\text{MeO}_4$  tetrahedron using the Slater-Koster parametrization [16], if the coordinate system is chosen as shown in Fig. 4.

	$p_\sigma$	$p_1$	$p_2$
$d_{xy}$	$\frac{1}{\sqrt{3}} t_{pd\sigma}$	0	$\frac{\sqrt{2}}{3} t_{pd\pi}$
$d_{yz}$	$\frac{1}{\sqrt{3}} t_{pd\sigma}$	$\frac{-1}{\sqrt{6}} t_{pd\pi}$	$\frac{-1}{3\sqrt{2}} t_{pd\pi}$
$d_{zx}$	$\frac{1}{\sqrt{3}} t_{pd\sigma}$	$\frac{1}{\sqrt{6}} t_{pd\pi}$	$\frac{-1}{3\sqrt{2}} t_{pd\pi}$

so that one may think that in the case of the regular tetrahedra the  $t_{2g}/t_{2g}$  exchange with a good precision can be described solely by the superexchange between the  $a_{1g}$  orbitals via the  $p_\sigma$  orbital.

Since  $J_4$  is considerably larger than other in-plane exchange couplings it fixes the directions of the spin moments on two out of three tetrahedral Fe sites, i.e. makes spins of these Fe ions antiparallel. The exchange constants  $J_3$  and  $J_5$  describing coupling between the octahedral  $\text{Fe}_o$  and tetrahedral  $\text{Fe}_t$  ions are noticeably smaller than  $J_4$  for the pair of the tetrahedral  $\text{Fe}_t$ . There are two reasons for that.

First of all the angle of the  $\text{Fe}_t\text{-O-Fe}_o$  bond is far from  $180^\circ$  (the  $\text{Fe}_t\text{-O-Fe}_t$  bond angle is exactly  $180^\circ$ ). If it was  $\sim 180^\circ$  then the superexchange between the  $\text{Fe}_t$   $t_{2g}$  and  $\text{Fe}_o$   $e_g$  states via the O  $p_\sigma$  orbital would be of order of the  $t_{2g}/t_{2g}$  superexchange in the pair of the tetrahedral  $\text{Fe}_t$  ions (the number of active orbitals (two  $e_g$  orbitals) of the octahedral  $\text{Fe}_o$  will be smaller than in the tetrahedral case (three  $t_{2g}$  orbitals), but they will be directed exactly to the oxygens). However this is not the case. There are two types of the tetrahedron-octahedron bonds in  $\text{Bi}_2\text{Fe}_4\text{O}_9$  structure: one with the  $\text{Fe}_t\text{-O-Fe}_o$  angle  $\alpha_1 \sim 120^\circ$  and another with  $\alpha_2 \sim 130^\circ$  (see Fig. 1). The first one provides exchange coupling  $J_5$ , while the second -  $J_3$ . Since  $\alpha_{1,2}$  are far from both  $180^\circ$  and  $90^\circ$ , the  $t_{2g}/t_{2g}$  and  $t_{2g}/e_g$  superexchanges should be comparable. The direct calculation shows that for the  $120^\circ$  bond:  $J_5^{t_{2g}/t_{2g}} = 8$  K and  $J_5^{t_{2g}/e_g} = 8$  K, while for the  $130^\circ$  bond  $J_3^{t_{2g}/t_{2g}} = 13$  K and  $J_3^{t_{2g}/e_g} = 15$  K. Note, that the contribution coming from the  $e_g$  orbitals is surprisingly almost the same for these two exchange pairs:  $J_5^{e_g/e_g} = 7$  K and  $J_3^{e_g/e_g} = 8$  K.

The second important difference between exchanges in the  $\text{Fe}_t\text{-Fe}_t$  and  $\text{Fe}_t\text{-Fe}_o$  pairs is in the Fe-O bond distance. In the case of two tetrahedral  $\text{Fe}_t$  ions both  $\text{Fe}_t\text{-O}$  bond distances are  $d(\text{Fe}_t - \text{O}) = 1.81$  Å. While for the  $\text{Fe}_t\text{-Fe}_o$  pair in the case of the bond angle  $\alpha_1 = 120^\circ$  ( $J_5$ ):  $d(\text{Fe}_t - \text{O}) = 1.91$  Å and  $d(\text{Fe}_o - \text{O}) = 2.03$  Å, while for  $\alpha_2 = 130^\circ$  ( $J_3$ ):  $d(\text{Fe}_t - \text{O}) = 1.85$  Å and  $d(\text{Fe}_o - \text{O}) = 1.97$  Å. The  $\text{Fe}_o - \text{O}$  bond distances are larger than  $\text{Fe}_t - \text{O}$  since the ionic radius of the  $\text{Fe}^{3+}$  is larger in the octahedral coordination than in tetrahedral ( $R_{HS}^{IV}(\text{Fe}^{3+}) = 0.49$  Å while  $R_{HS}^{VI}(\text{Fe}^{3+}) = 0.645$  Å). [19]

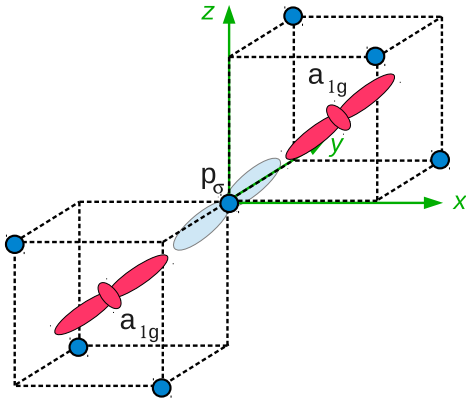


FIG. 4: (color online). The sketch illustrating the strongest exchange coupling between  $a_{1g}$  orbitals on two tetrahedral  $\text{Fe}_t$  ions via the  $p_\sigma$  (light blue color) orbital, directed to the centers of tetrahedra. Oxygen ions are blue balls.

It is rather complicated to find analytically the bond and angle dependence of all exchange constants due to the strongly distorted crystal structure and many active (magnetically) orbitals in  $\text{Bi}_2\text{Fe}_4\text{O}_9$ . We performed such calculations for the  $t_{2g}/e_g$  contribution to the exchange coupling between the octahedral and tetrahedral Fe ions with the  $130^\circ$  and  $120^\circ$   $\text{Fe}_t\text{-O-Fe}_o$  bonds angles. Within the 4th order of the perturbation theory and using approximations that as it was shown above the  $\text{Fe}_t\text{-O}$  hoppings occur only via the  $p_\sigma$  orbital and that they depend only on the  $\text{Fe}_t\text{-O}$  bond distance one may find that

$$J_{to}^{t_{2g}-e_g} \sim \sum_i \frac{(t_{p_\sigma a_{1g}}^{tet})^2 (t_{p_\sigma e_g^i}^{oct})^2}{U \Delta_{CT}^2} \sim \sum_i C (t_{p_\sigma e_g^i}^{oct})^2, \quad (6)$$

where  $i$  numerates the  $e_g$  orbitals of the octahedral  $\text{Fe}_o$ . The  $t_{p_\sigma e_g^i}$  can be estimated using the Slater-Koster coefficients and atomic positions of the Fe and O ions. Then if one takes into account only the angle dependence of the hopping matrix elements  $J_{to}^{t_{2g}/e_g}(130^\circ)/J_{to}^{t_{2g}/e_g}(120^\circ) = 1.45$ . The bond length dependence can be found using the Harrison parametrization of the  $pd$  hopping integrals ( $t_{pd} \sim \frac{1}{r^{3.5}}$ ), [17] which gives  $J_{to}^{t_{2g}/e_g}(130^\circ)/J_{to}^{t_{2g}/e_g}(120^\circ) = 1.22$ . Taking into account both mechanisms (the angle and bond length dependence) one finds that this ratio is  $\sim 1.8$ , which agrees reasonably with the same ratio, obtained in the LSDA+U calculation, which equals 1.9.

Calculated exchange constants are in qualitative agreement with the estimations made in Ref. 7. All exchange constants in the  $ab$  plane are antiferromagnetic and the ratio of two tetrahedral-octahedral exchange constants  $J_3/J_5 \approx 1.6$  (2.15 in Ref. 7). Because of the difference between  $J_3$  and  $J_5$   $\text{Bi}_2\text{Fe}_4\text{O}_9$  cannot be considered as a perfect realization of the Cairo pentagonal lattice, [7] but still the deviations are not so strong, and it makes sense to compare our situation with that of the ideal lattice.

There are only two exchange constants in the perfect version of this lattice  $J_4$  and  $J_3 = J_5$ . The model study of the magnetic properties of the ideal Cairo pentagonal lattice shows that its ground state corresponds to the orthogonal spin order, if  $J_3/J_4 < \sqrt{2}$ . [1] According to our calculations both  $J_5/J_4 \approx 0.32$  and  $J_3/J_4 \approx 0.49$  are less than  $\sqrt{2}$ , and hence the ground state is also expected to be described by the orthogonal spin order, exactly as it was observed experimentally. [7]

There are two types of the exchange constants, which couple the octahedral  $\text{Fe}_o$  ions along the  $c$  axis. The first one,  $J_1$  ( $\text{Fe}_o\text{-Fe}_o$  bond distance 2.90 Å), actually has to be considered as a part of the pentagonal lattice (see Fig. 2). This constant is antiferromagnetic and equals  $J_1=10$  K, almost a half of one of the in-plane exchanges ( $J_5$ ). It brings additional (to pentagonal) frustration in the spin system, since there are four antiferromagnetic triangles linked with each pentagon, see Fig. 2. The second interplane exchange,  $J_2=12$  K ( $\text{Fe}_o\text{-Fe}_o$  bond distance 3.10 Å), is antiferromagnetic as well and couples different pentagonal planes with each other.

#### IV. CONCLUSIONS

In the present paper we carried out the band structure calculations of  $\text{Bi}_2\text{Fe}_4\text{O}_9$  and found that it must be classified as a charge transfer insulator. The investigation of the exchange constants shows that this compound cannot be considered as a perfect realization of the Cairo pentagonal lattice. First of all there are two different exchange parameters between the tetrahedral and octahedral Fe ions. Second the interplanar exchange coupling additionally frustrates the system. The exchange constants along the  $c$  axis are not negligibly small and exceed 50% of one of the intraplanar exchange ( $J_5$ ). However, in spite of these findings  $\text{Bi}_2\text{Fe}_4\text{O}_9$  still demonstrates nearly orthogonal spin order below  $T_N$  [7] in accordance with the results obtained in Ref. 1, where the study of the perfect Cairo pentagonal model was performed. This is due to the fact that both exchange parameters between the tetrahedral and octahedral Fe ions ( $J_3$  and  $J_5$ ) are much smaller than the magnetic coupling between the tetrahedral Fe sites ( $J_4$ ). Strong  $J_4$  makes the spins on two out of three tetrahedral sites antiparallel, while the ratio between  $J_3$  and  $J_5$  define the angles between spin moments on the rest one tetrahedral and two octahedral Fe sites. The microscopic analysis shows that the largest contribution,  $\sim 70\%$ , to  $J_4$  comes from the coupling between the  $t_{2g}$  orbitals on different sites. The deviations from the perfect Cairo pentagonal model are expected for more subtle characteristics such as e.g., low energy excitation spectra.

## V. ACKNOWLEDGMENTS

The authors thank Prof. P. Radaelli, who drew our attention on this system. This work is supported by the Russian Foundation for Basic Research via RFFI-

13-02-00374, RFFI-13-02-00050, RFFI-12-02-31331, the Ministry of education and science of Russia (grants 12.740.11.0026, MK-3443.2013.2, 14.A18.21.0889). The part of the calculations were performed on the “Uran” cluster of the IMM UB RAS.

- 
- [1] I. Rousochatzakis, A. Läuchli, and R. Moessner, *Physical Review B* **85**, 104415 (2012), ISSN 1098-0121, URL <http://link.aps.org/doi/10.1103/PhysRevB.85.104415>.
- [2] D. Shechtman, I. Blech, D. Gratias, and J. Cahn, *Physical Review Letters* **53**, 1951 (1984), ISSN 0031-9007, URL <http://link.aps.org/doi/10.1103/PhysRevLett.53.1951>.
- [3] A. M. Abakumov, D. Batuk, A. a. Tsirlin, C. Prescher, L. Dubrovinsky, D. V. Sheptyakov, W. Schnelle, J. Hadermann, and G. Van Tendeloo, *Physical Review B* **87**, 024423 (2013), ISSN 1098-0121, URL <http://link.aps.org/doi/10.1103/PhysRevB.87.024423>.
- [4] a. K. Singh, S. D. Kaushik, B. Kumar, P. K. Mishra, A. Venimadhav, V. Siruguri, and S. Patnaik, *Applied Physics Letters* **92**, 132910 (2008), ISSN 00036951, URL <http://link.aip.org/link/APPLAB/v92/i13/p132910/s1>.
- [5] A. Poghossian, H. Abovian, P. Avakian, S. Mkrtchian, and V. Haroutunian, *Sensors and Actuators B: Chemical* **4**, 545 (1991), ISSN 09254005, URL [http://dx.doi.org/10.1016/0925-4005\(91\)80167-I](http://dx.doi.org/10.1016/0925-4005(91)80167-I).
- [6] A. G. Tutov, I. E. Mylnikova, N. N. Parfenova, V. A. Bokov, and S. A. Kizhaev, *Sov. Phys. Solid State* **6**, 963 (1964).
- [7] E. Ressouche, V. Simonet, B. Canals, M. Gospodinov, and V. Skumryev, *Physical Review Letters* **103**, 267204 (2009), ISSN 0031-9007, URL <http://link.aps.org/doi/10.1103/PhysRevLett.103.267204>.
- [8] K. Momma and F. Izumi, *J. Appl. Crystallogr.* **44**, 1272 (2011).
- [9] O. K. Andersen and O. Jepsen, *Phys. Rev. Lett.* **53**, 2571 (1984), URL <http://link.aps.org/doi/10.1103/PhysRevLett.53.2571>.
- [10] U. von Barth and L. Hedin, *Journal of Physics C: Solid State Physics* **5**, 1629 (1972), URL <http://iopscience.iop.org/0022-3719/5/13/012>.
- [11] V. Anisimov, F. Aryasetiawan, and A. Lichtenstein, *J. Phys.: Condens. Matter* **9**, 767 (1997), URL <http://iopscience.iop.org/0953-8984/9/4/002>.
- [12] S. V. Streltsov and N. A. Skorikov, *Phys. Rev. B* **83**, 214407 (2011), ISSN 1098-0121, URL <http://link.aps.org/doi/10.1103/PhysRevB.83.214407>.
- [13] A. J. Hearmon, F. Fabrizi, L. C. Chapon, R. D. Johnson, D. Prabhakaran, S. V. Streltsov, P. J. Brown, and P. G. Radaelli, *Phys. Rev. Lett.* **108**, 237201 (2012).
- [14] A. Liechtenstein, V. Gubanov, M. Katsnelson, and V. Anisimov, *Journal of Magnetism and Magnetic Materials* **36**, 125 (1983).
- [15] J. Zaanen, G. Sawatzky, and J. Allen, *Physical Review Letters* **55**, 418 (1985), ISSN 0031-9007, URL <http://link.aps.org/doi/10.1103/PhysRevLett.55.418>.
- [16] J. C. Slater and G. F. Koster, *Phys. Rev.* **94**, 1498 (1954), URL [http://prola.aps.org/abstract/PR/v94/i6/p1498\\_1](http://prola.aps.org/abstract/PR/v94/i6/p1498_1).
- [17] W. Harrison, *Elementary Electronic Structure* (World Scientific, Singapore, 1999).
- [18] These are not true trigonal orbitals, which are defined in the chosen coordinate system as  $\phi = \frac{1}{\sqrt{3}}(xy + e^{i\frac{2\pi}{3}n}xz + e^{-i\frac{2\pi}{3}n}yz)$ , with  $n = 0$  corresponding to  $a_{1g}$  and  $n = 1, -1$  to  $e_g^\pi$ .
- [19] R. D. Shannon, *Acta Crystallographica Section A* **32**, 751 (1976).